Parallel Imaging Using a 3D Stack-of-Rings Trajectory

H. H. Wu[1,2], M. Lustig[2,3], and D. G. Nishimura[2]

[1]Cardiovascular Medicine, Stanford University, Stanford, CA, United States, [2]Electrical Engineering, Stanford University, Stanford, CA, United States, [3]Electrical Engineering and Computer Science, University of California at Berkeley, Berkeley, CA, United States

Introduction: The 3D stack-of-rings non-Cartesian *k*-space trajectory, based on the 2D concentric rings [1−5], enables robust and time-efficient magnetization-prepared imaging due to its unique circularly symmetric sampling nature [4, 5]. At the same time, this circular symmetry enables a time-efficient retracing acquisition that can resolve off-resonance effects and perform fat/water separation [3−5]. In this work, we present an efficient parallel imaging strategy for the 3D stack-of-rings trajectory to further enhance its flexible trade-offs between image quality and scan time. Non-Cartesian sampling and parallel imaging [6−8] are two complementary acceleration methods; combining the two can potentially enable a great reduction in scan time. However, the general problem of performing parallel imaging with an arbitrary sampling trajectory is computationally demanding [7]. Once again, due to its distinct geometry, parallel imaging reconstruction for the 3D stack-of-rings trajectory can be decomposed directly into a series of 2D Cartesian sub-problems, which can be solved very efficiently. Our approach thus combines the acceleration from both non-Cartesian sampling and parallel imaging in an efficient and easily deployable algorithm.

Methods: The 3D stack-of-rings trajectory encodes (k_x, k_y) with a set of 2D concentric rings and covers k_z with conventional slice encoding, already enabling a 2-fold scan-time reduction with respect to 3D Cartesian encoding [1−5]. In addition, efficient parallel imaging reconstruction is possible for the 3D stack of rings by recognizing that the dataset can be reformatted as a collection of "spoke-planes" (Fig. 1a) which cut through the rings acquisition along full-diameter spokes and contains data points that lie directly on 2D Cartesian grids. Parallel imaging reconstruction for the 3D stack of rings can thus be decomposed directly into a series of fast 2D Cartesian reconstructions for each spoke-plane. After the missing data points are filled out for each spoke-plane and coil [8], a Fourier transform is taken along k_z, followed by a series of 2D gridding reconstructions for each (k_x, k_y)-plane. Data from multiple coils are combined using a sum-of-squares approach.

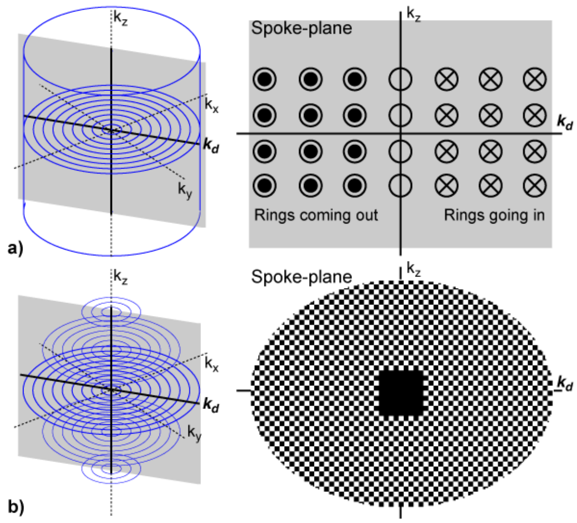

Fig. 1. (a) Parallel imaging reconstruction for the 3D stack of rings can be broken down into a series of 2D Cartesian problems for "spoke-planes" that cut through the rings along a full-diameter spoke (k_d). Data points lie directly on a 2D Cartesian grid in each spoke-plane. **(b)** For our experiments, the 3D stack of rings are acquired with spherical coverage in *k*-space. An R = 2 checkerboard undersampling pattern with calibration region (**black**: sampled) is applied retrospectively to demonstrate parallel imaging reconstruction.

Experiments: Setup: 3D head scans were performed on a GE Signa 1.5 T Excite system using an 8-channel head coil. The FOV was 24x24x18 cm^3 and matrix size was 240x240x180 (120 rings of 472 samples/2π in (k_x, k_y)). Each ring was acquired over 3 revolutions to enable fat/water separation [3−5]. Spherical coverage was implemented (Fig. 1b) [5] and this 3D stack-of-rings trajectory was incorporated into an IR-SPGR sequence that produced high white/gray matter contrast [4, 5]. Total scan time for the fully-sampled dataset was 7 min. This dataset was reformatted as 236 spoke-planes of 239x180 points each and retrospectively undersampled with a checkerboard pattern of reduction factor R = 2 (Fig. 1b). GRAPPA-based reconstruction [8] was performed for each spoke-plane using a fully-sampled central region of 17 rings x 32 slices (33x32 in each spoke-plane) for calibration and a 5x5 interpolation kernel. Results: Shown in Fig. 2 are representative head images (water images) obtained by using a fully-sampled reconstruction (Fig. 2a), a zero-filled reconstruction of the undersampled dataset (Fig. 2b), and by using the proposed parallel imaging reconstruction algorithm for the undersampled dataset (Fig. 2c). Aliasing is seen in the zero-filled reconstructions, while the parallel imaging reconstructions exhibits minimal residual aliasing and closely match the fully-sampled reconstructions.

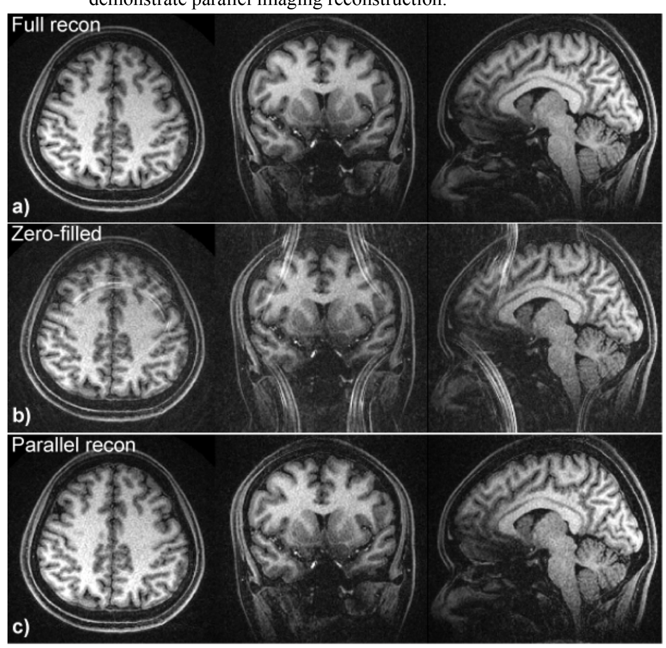

Fig. 2. Representative axial, coronal, and sagittal cuts from the same 3D head scan using **(a)** fully sampled reconstruction, **(b)** undersampling with zero-filled reconstruction, and **(c)** undersampling with parallel imaging reconstruction.

Discussion: The 3D stack-of-rings trajectory has a distinct sampling geometry that allows its parallel imaging reconstruction to be broken down into a series of fast 2D Cartesian calculations. Experimental results demonstrate that a 2-fold acceleration in scan time (R = 2) can be achieved on top of the 2-fold time savings inherently offered by the rings. This means that the fat-water-separated 3D head scan would only take 3.5 minutes. In addition to the uniform undersampling example shown, it may be possible to design the 3D stack-of-rings undersampling pattern to fully utilize coil sensitivity encoding in all three spatial dimensions. While the spoke-plane decomposition enables a fast reconstruction, the azimuthal neighbors on multiple spoke-planes currently are not used to estimate missing data. In the future, we will compare our current approach to a fully 3D parallel imaging reconstruction method and explore higher undersampling reduction factors.

References: [1] Matsui S, et al., JMR 1986; 70: 157-162. [2] Wu HH, et al., MRM 2008; 59: 102-112. [3] Wu HH, et al., MRM 2009; 61: 639-649. [4] Wu HH, et al., *Proc. 17th ISMRM*, p.2647, 2009. [5] Wu HH, et al., MRM (in press). [6] Pruessmann KP, et al., MRM 1999; 42: 952-962. [7] Pruessmann KP, et al., MRM 2001; 46: 638-651. [8] Griswold MA, et al., MRM 2002; 47: 1202-1210.